Integrated High Performance Microfluidic Organic Analysis Instrument for Planetary and Space Exploration

Anna L. Butterworth[*1], *Matin Golozar*[2], *Zachary Estlack*[3], *Jeremy McCauley*[1], *Jungkyu Kim*[3] *and Richard A. Mathies*[1,2]

[1]Space Sciences laboratory, University of California Berkeley, Berkeley CA 94720, USA

[2]Chemistry Department, University of California, Berkeley CA 94720, USA

[3]Department of Mechanical Engineering, University of Utah, Salt Lake City, UT 84112, USA

*Address correspondence to Anna Butterworth at butterworth@berkeley.edu

ABSTRACT: The exploration of our solar system to characterize the molecular organic inventory will enable the identification of potentially habitable regions and initiate the search for biosignatures of extraterrestrial life. However, it is challenging to perform the required high-resolution, high-sensitivity chemical analyses in space and in planetary environments. To address this challenge, we have developed a Microfluidic Organic Analyzer (MOA) instrument that consists of a multilayer Programmable Microfluidic Analyzer (PMA) for fluidic processing at the microliter scale coupled with a microfabricated glass capillary electrophoresis (CE) wafer for

separation and analysis of the sample components. Organic analytes are labeled with a functional group-specific (e.g. amine, organic acid, aldehyde) fluorescent dye, separated according to charge and hydrodynamic size by capillary electrophoresis (CE), and detected with picomolar sensitivity using laser-induced fluorescence (LIF). Our goal is a sensitive automated instrument and autonomous process that enables sample-in to data-out performance in a flight capable format. We present here the design, fabrication and operation of a Technology Development Unit (TDU) that meets these design goals with a core mass of 3 kg and a volume of < 5 L. MOA has a demonstrated resolution of $2x10^5$ theoretical plates for relevant amino acids using a 15-cm long CE channel and 467 V/cm. The LIF sensitivity is better than 100 pM or 0.01 ppb enabling detection of biosignatures in the most challenging model environments on Earth; MOA is an ideal choice for probing for biosignatures at potentially habitable destinations on icy moons such as Europa and Enceladus, and on Mars.

KEYWORDS

Capillary Electrophoresis; Amino acids; Biosignatures; Ocean Worlds; Enceladus; Europa; Mars

INTRODUCTION

Performing in situ, high-performance chemical and biochemical analyses is a critical capability for conclusively exploring our solar system for chemical indications of habitable or inhabited environments[1]. Thus far, in situ extraterrestrial chemical exploration has focused on Mars due to its accessibility. The pioneering 1976 Viking landers performed pyrolysis Gas Chromatography-Mass Spectrometry (GC-MS) chemical analyses of Mars surface and subsurface samples and concluded that resident or accumulated organic materials must be below a few parts per billion.[2, 3] The Mars Exploration Rovers conducted extensive surface investigations with imaging and

mineral spectroscopy but did not accommodate direct chemical analyses of the Martian surface.[4] The larger Mars Science Laboratory Curiosity rover deployed the Sample Analysis at Mars (SAM)[5] instrument including a pyrolysis GC-MS instrument. SAM analyses of surface sedimentary samples at Gale Crater detected 150 ng/g chlorobenzene and up to 70 ng/g dichloroalkanes.[6] SAM derivatization experiments detected 4 µg/g benzoic acid and 12 µg/g ammonia, but did not detect any amino acids above the sensitivity limit of 10 ng/g of sample .[7] The current Mars 2020 Perseverance Rover is using a non-contact UV fluorescence and Raman scattering instrument (SHERLOC) to characterize minerals and search for organics above 10 µg/g in drilled surface samples.[8]

While these missions demonstrate significant progress in the chemical exploration of our solar system, there is growing interest in other astrobiological locations including the icy moons of Saturn (e.g. Enceladus) and of Jupiter (e.g. Europa) that are more difficult to access and have more challenging operational environments;[9] their meaningful exploration will require high-performance, lower-mass flight capable instrumentation with higher sensitivity than thus far deployed.[10–13] The science case for Enceladus sets the goal of searching for potential biosignatures in its plumes and on the surface as well as quantifying the habitability of the ocean.[14, 15] The recently presented OrbiLander flagship mission concept[16] strongly makes this case and indicates the instrument capabilities that will be needed to address these science objectives. For example, wet chemistry sample processing yields significantly higher analyte sensitivity compared to GC-MS; while capillary electrophoresis (CE) with laser-induced fluorescence is capable of part-per trillion sensitivity (10^{-15} mole detection), achieving 1000-fold improvement in detection sensitivity over current flight GCMS instrumentation for detection of organic biosignatures.[18, 19] To complement enhanced analytical capabilities, missions will require

collection of surface or plume samples to enable these higher sensitivity wet chemistry-based trace organic biosignature analyses.[20]

Over the past 30 years, microfluidic technology has advanced rapidly,[21, 22] demonstrating 1000-fold (mL to μL) volume reductions, integrated fluid handling, high-resolution separation and high sensitivity laser-induced fluorescence (LIF) detection.[23, 24] Microfluidic systems are insensitive to gravity and enable precise processing of small volumes of limited samples, which is ideal for planetary exploration. Electrophoresis does not require ionization, fragmentation of organic molecules, nor a flowing separation phase. Integrated CE techniques therefore enable straightforward instrument development,[25] without the need for coupling GC or LC systems to an MS for gas phase ionization.

The unique capabilities of microfabricated glass capillary electrophoresis have been exploited to develop analyses of organic and biosignature molecules including amines, amino acids, carboxylic acids, aldehydes, ketones, thiols and amino sugars by ourselves and others.[18, 26–31] While the majority of this research was performed using laboratory-based instrumentation, portable prototype microfluidic CE instruments have been developed and field-tested successfully in a variety of terrestrial locations[25, 32, 33] and on challenging field samples.[32, 34] However, these important achievements are still far from the development of a flight-ready design that enables high performance analyses autonomously deployed in solar system exploration.

Our present goal is to design, fabricate, and demonstrate a compact, low-mass microfluidic organic analyzer in a flight-capable format that offers the sensitivity and resolution necessary for meaningful organic results concerning habitability and the possible presence of biosignatures in extraterrestrial environments.[11] Figure 1 provides a schematic overview of our Microfluidic

Organic Analyzer (MOA) instrument analysis procedure. The organic analytes are labeled with a reactive fluorescent dye that is specific for typical organic functional groups following the concepts originally presented by Skelley et al.[35] The analytes are solubilized, labeled, and processed utilizing the PMA (Programmable Microfluidic Analyzer), consisting of a pneumatically actuated microvalve array developed by Kim et al.[36] The labeled analytes are separated using an integrated microfabricated glass capillary electrophoresis channel and detected using a compact optimized LIF detection system.[19, 37] We describe the fabrication, operation, and performance of this unique instrument and demonstrate its ability to perform organic analyses on challenging real-world samples that are relevant for Enceladus, Europa, and the biologically special regions on Mars.

EXPERIMENTAL SECTION

Figure 2 presents a schematic of components in the MOA comprising the fabricated flight design instrument. In overview, the exploded wafer stack illustrated in Figure 2 consists of the polydimethylsiloxane (PDMS) pneumatic layer, the PDMS fluidic layer and the bonded glass CE wafers. Once assembled, this 100 mm diameter wafer stack is mounted in a 3D-printed titanium manifold, containing 39 three-way latching solenoid valves (custom part, The Lee Company) that route pressure or vacuum to the wafer device microvalves. The manifold lid provides electrical interfaces to the CE system and encloses the pressure vessel, enabling operation in a vacuum environment. A miniature confocal laser induced fluorescence (LIF) system (5 cm in length) provides analyte detection. The assembled unit is compact < 5 L and low mass, 3 kg. Detailed design and fabrication of the instrument are discussed in the following section.

CE wafer fabrication: The fabrication of high-quality glass capillary electrophoresis wafer stacks is performed using well-developed photolithographic glass wet etching techniques as updated recently by Golozar et al.[37] In brief, Borofloat glass wafers (100 mm dia., 0.7 mm thick) are cleaned using a standard wafer cleaning protocol.[38] They are then coated with a 2000 Å of amorphous silicon (a-Si) using a Low-Pressure Chemical Vapor Deposition (LPCVD) furnace followed by deposition of a 2 μm layer of positive photoresist through spin coating and a soft bake at 120^{o} C for 2.5 min to semi-harden the photoresist. The uniformity and lack of pinholes in the amorphous-Si layer is critical for making a defect free device. The microchannels are then imaged through a chrome mask onto the photoresist and a-Si layers using standard UV lithography and SF_6 plasma etch, respectively. Hydrofluoric acid (49%) is used to isotropically etch the glass wafer to produce 110 μm wide and 30 μm deep channel trenches. The overall electrophoresis channel length is 15 cm but the channel is folded using a hyperturn geometry to avoid racetrack broadening of the electrophoresis zones.[39] The 5-mm long Sample and Waste arms are placed 5 mm from the Anode in the standard crossed T format so that the edge of each reservoir is 4.2 mm from the intersection. The remaining photoresist and a-Si is removed using acetone and SF_6 plasma, respectively. Access holes are drilled in a separate blank Borofloat glass wafer (100 mm dia., 1.5 mm thick) on a CNC mill at 10,000 rpm under water. Finally, the etched and drilled wafers are thoroughly cleaned and thermally bonded together at 668^{o} C for 6 hours to obtain a microfluidic CE chip. Typical yields were 90% with refined procedures; the most prevalent flaw was slight misalignment of wafers during the bonding step resulting in deselection.

PMA fabrication: The PMA is fabricated using conventional soft lithography techniques with additional steps to ensure consistent yield and integration as detailed by Estlack et al.[40] First, two SU-8 molds, one defining the pneumatic channels (80 μm thick) and another for the fluidic channels (50 μm thick), are created. The pneumatic mold is secured in an aluminum tray for thickness consistency and the fluidic mold is coated with Parylene-C to aid in PDMS release. PDMS is poured into the pneumatic mold to 4.5-mm depth, while the fluidic mold is spin coated with PDMS, resulting in a layer ~200 μm thick. Each PDMS layer is cured on a hotplate set to 45º C overnight. The low temperature and long cure time is used to avoid shrinkage so that PMA can be integrated with a glass μCE chip without alignment tolerance issues. The PDMS layers are removed from their respective molds and all interfacing ports, including pneumatic ports and the interconnection ports for the μCE chip, are punched out using a biopsy punch mounted in a drill press to ensure orthogonality of the punched holes. In the fully assembled device, these holes define the fluid wells and pneumatic connections. Next, the pneumatic and fluidic layers are bonded together by exposing both layers to oxygen plasma, aligning and bringing two layers into contact, and then placing the layers on a hotplate at 65º C for 30 minutes completing the PMA fabrication.

The next step is to bond the PMA to the glass μCE chip. All gates of the microvalves (indicated in **Figure 3**) are first passivated with trichloro(1H,1H,2H,2H-perfluorooctyl) silane (PFTCS) by microcontact printing to prevent sticking.[41] In brief, a shadow mask is created by cutting out the locations of the microvalves on vinyl tape and placing it over a blank PDMS slab. The masked slab is placed in a vacuum chamber (-80 kPa) with 100 μL of PFTCS for 30 minutes for vapor deposition of PFTCS. After PFTCS deposition, the mask is removed, and the slab is placed in a motorized alignment system with the PMA held by a vacuum chuck. The motorized

system along with a digital microscope are used to align the slab and the microvalve gate on the PMA and press them together. The slab and PMA are then placed on a hotplate at 150º C for 30 minutes to allow the PFTCS to be transferred to the microvalve gates. The fully assembled PMA and the μCE glass surfaces are plasma treated, then aligned using an interface holder with location posts and pressed together. The final assembly is placed onto a hotplate at 65º C for 30 minutes to complete bonding.

PMA Operation: The pneumatic microvalves in our wafer device operate by applying either pressure (48±2 kPa) or vacuum (-70 kPa) to selected pneumatic access ports for fluidic manipulation, each controlled by a latching solenoid valve. When applying vacuum, the microvalve membrane deflects to the top of the pneumatic chamber, pulling in a volume of fluid that can then be pushed out when the port switches to pressure. As shown in Figure 3, an array of 12 microvalves (1.5 mm in diameter) constitutes the central processor microvalves (CPM), with four (or one case five) inputs to each valve, surrounded by 15 2-port routing gate valves (1 mm diameter) that route fluid from the CPM to the desired fluid well location or the reverse. The CPM 4-way microvalve displacement volume is 80 nL and the smaller 2-way gate valve displacement volume is 20 nL.

The CPM microvalves and routing gates and six CE port gates are individually actuated, while the 30 reagent well gates are controlled by row-column addressing, requiring only one solenoid input per row and one per column. The order and timing of the microvalve actuations in a sequence defines a pump cycle, which moves fluid from a source, routed through a gate into the CPM and out through a specified gate to a fluid destination. The actuation sequences are generated by a program written in Python, which converts the fluid source, destination, and the

CPM filling and emptying speeds into automated actuation sequences, as illustrated in detail in Figure S1 for metered and peristaltic pumping modes described below.

In *metered pumping* mode, a specified number of CPM valves open sequentially with a relatively long time between individual valve operations, to displace a fixed volume. The longer time spent open for CPM valves ensured stable volume transfer, with 850±15 nL (2% variation) in total volume displaced per pump cycle. Alternating sources while delivering to a common destination performs mixing of two fluids with a volume ratio defined by the total number of pump cycles for each source. The spreadsheet in Table S1 indicates how multiple labeling, mixing and dilution program steps are used to build a precise automated fluidic protocol required for a specified experiment.

In *peristaltic pumping* mode, a fluid bolus is pumped as a wave flowing through a short path in the CPM, by rapidly switching valves states as shown in Figure S1. Multiple fast cycles transfer a smaller volume per cycle than metered pumping but achieve a greater overall volumetric flowrate. There are two options for peristaltic pumping: a *Fast Pump* sequence for single-source transfers on-chip is effective for filling CE wells with labeled sample. The *Off-chip* sequence is used for ingesting fluid from a single off-chip source using pressure-assisted displacement pumping to increase the overall flow rate by allowing only a brief (< 1 s) "leak" of pressure-driven flow per cycle, while the positive displacement pumping ensures against uncontrolled flow.

Confocal Laser-Induced Fluorescence Detection System:

The miniature flight-like confocal detection system comprised a 405 nm diode laser for excitation (Thorlabs DL5146-101), 405 nm bandpass excitation filter (Chroma ZET405/20x),

425 nm long-pass dichroic mirror (Chroma ZT405rdc), dual band pass emission filter (ZET405/467nm), 0.6 numerical aperture objective, and a solid-state photomultiplier tube module (μPMT – Hamamatsu H12405). The compact optical unit is 5-cm long and two detectors fit inside the instrument manifold ring, one for each CE channel (**Figure 2)**. The detector buffer blank noise, determined by water Raman (OH stretch 470 nm maximum) shot noise, was measured equivalent to 25 pM Pacific Blue succinimidyl ester (PBSE) at 10 mW laser power, 55 μm beam spot in the channel, and a μPMT gain setting of 0.8 V control voltage (7 x 10^5 optical gain). The PBSE LOD (S/N 3) was determined by measuring fluorescence intensity of 1 nM PBSE at different μPMT gain settings and found to be 50 pM.

Integrated and automated amino acid analysis:

Reagent stocks were prepared as follows: Purified water was prepared by irradiating 18.2 MΩ water (Direct-Q, MilliporeSigma) for 12 hours with 254 and 185 nm UVC lamp (Black Magic 3D: UVC-25W-OZONE-WT), followed by distillation and a second irradiation to minimize background amino acids. Borate buffer (300 mM) was prepared in purified water (1.43 g sodium tetraborate, molecular weight: 381.37 g/mol, in 50 mL water). Pacific Blue succinimidyl ester (PBSE, ThermoFisher) was dissolved in dry acetone and aliquoted to deposit 1 nanomole PBSE in rinsed, dried Eppendorf tubes and stored in the freezer. Amino acids were dissolved in purified water and combined to make a stock test mixture containing 1 mM Arg, His, Leu, Val, γABA, S, βAla, Ala, Gly, and 2 mM Iva, Glu, and Asp.

An automated analysis of a mixture of amino acids was performed to demonstrate the utility and abilities of the MOA instrument. Starting with the stored dry microfluidic device, the first step was to prime the CPM and gate valves with water followed by degassing by holding the

CPM valves open and removing any remaining bubbles through the PDMS membrane. Priming took approximately 4 minutes to complete from a user-defined water source location. The steps were automated and flexible and details are shown in SI and Figure S2.

The following sequence was used to load the chip for an experiment: Stock amino acid test mixture was diluted to 100 nM Arg in water and 10 µL placed in *B1*; 1 nanomole dry PBSE dye was dissolved in 10 µL sodium borate (60 mM pH 9.2) and placed in *B2*; and 100 µL 30 mM borate pH 9.2 CE running buffer was loaded into a large volume well, *B6* (**Figure 3**). The automated experiment commenced by mixing dye in buffer and the amino acid sample solution 1:1, by alternating 10 *metered pumping* cycles from B1 and B2 to "large volume" *LV1* well, (**Figure 4, Panels A and B)**, Mixing 7.5 µL of each solution resulting in 13 µL labeling mixture (2 µL total dead volume). The automated mixing step was completed in 2 minutes.

Labeling conditions were 50 µM PBSE, 30 mM borate at pH 9.2, 50 nM arginine plus other test mixture amino acids totaling 700 nM, incubated at room temperature for 1 hour. During incubation, the CPM was rinsed by pumping 1X buffer from *B6* to *Waste*, refilled with buffer and degassed, while the µCE was prepared. The CE channel was conditioned by passing 1M HCl, 1M NaOH, purified water and finally 1X borate buffer through the channels. The four CE wells were filled with buffer (25 µL each well) and platinum electrodes inserted in each reservoir.

After the labeling reaction was complete, the automated sequence continued with a 2:3 dilution step combining 10 *metered pumping* cycles transferring labeled sample from *LV1* to *LV2* and 15 metered cycles of 1X buffer from *B6* to *LV2* completed in only 2.5 minutes. The overall dilution of the amino acid solution was 5X from sample to detector.

To fill the CE sample reservoir for separation, the CE sample port, *CS2,* was emptied, one metered pump cycle from *B6* primed the short channel to *CS2* (<1 μL dead volume), then labeled sample in *LV2* was pumped to *CS2* for CE-LIF analysis (**Figure 4, Panel C**). Using slower *metered* pumping, the transfer to *CS2* took 5 minutes, which has since been reduced to 1.5 minutes by implementing fast *peristaltic* pumping. CE-LIF injections were optimized for the worse-case slower transfer, which involves some diffusion of sample from the Sample well into the CE channel during transfer.

Capillary Zone Electrophoresis (CZE) separation was performed with automated switching of potentials at the CE Sample, Waste and Cathode electrodes with Anode at ground. To correct for the diffusion occurring during the sample transfer time, an electrokinetic clean-up step was performed by applying -1000 V at CE Sample and Waste electrodes for 60 s to clear diffused molecules from the injection cross. A pinched CE injection was then performed (-1000 V at CE-Waste for 40 seconds), followed by rapid (100 ms) switching to the separation conditions of field strength 467 V/cm (Cathode -7 kV, back bias -640 V at Sample and Waste). Fluorescence was detected by LIF at the detection point 5 mm before the Cathode. With the electrokinetic cleanup step, multiple repetitive CE-LIF runs could be performed, taking 3 minutes per separation.

Two additional comparison experiments were performed on the integrated μCE to verify performance: First, to compare labeling efficiency on-chip, a similar test mixture sample was prepared on the bench (labeled for 1.5 hrs), manually loaded into the *LV2* well, and pumped to the μCE for CE-LIF analysis as before. Second, to test the automated CE transfer step, the same bench-prepared sample was manually loaded directly in the CE sample port and run as before. The three resulting traces are shown in **Figure 5**.

RESULTS

Dynamic testing of the CPM showed that a 300 ms actuation time is sufficient to completely fill or empty the volume displaced during microvalve actuation in the metered pumping mode, resulting in 850±15 nL of net forward flow over a nine second cycle, which is equivalent to a volumetric flow rate of 5.67±0.1 μL/min. Figure 3 presents the flow profile of the metered pumping cycle, with each closing operation of the CPM valves producing a pulse in the instantaneous flow rate. The outlet microvalve first opens during the brief period of backflow preceding the onset of the peaks. In contrast, the fast-pumping peristaltic cycle using 10 kPa head pressure, 300 ms leak step, and 100 ms microvalve actuations (including 30 ms solenoid switching time), achieved significantly higher 10.80 ±0.12 μL/minute flow rates (N = 20). Off-chip pressure assisted pumping therefore provides precise, user-defined volume and delivery rates to any location on the chip without risk of overfilling the destination fluid reservoir. However, because the CPM microvalves are not completely filled or emptied during fast actuation, there is an increased risk of bubble formation during the sequence as air can be pulled through the gas permeable PDMS PMA structure.

Multiple PMA actuation sequences were developed to prepare the system for autonomous nanoliter fluid manipulation. First, a priming sequence was developed to fill the PMA with liquid. Initially, the PMA is filled with gas, which must be replaced with liquid from an on- or off-chip reservoir. **Figure S2** describes the general priming sequence. Briefly, the CPM valves are partially filled with liquid and then kept open for ~30 seconds. Since the microvalves are open under vacuum, the gas permeability of PDMS allows for gas present in the valve chamber to diffuse through the membrane to the actuating vacuum. After the 30 second degassing period, the CPM microvalves are used to fill the surrounding gate valves before they are left to degas

along with the CPM valves, this time for two minutes. A second core sequence is the mixing of two fluids to utilize for amino acid analysis depicted in **Figure 4**. Another mixing example is filling a reagent storage well with alternating food color dyes as demonstrated in **SI Video**.

After characterizing the PMA function, the automated, integrated labeling and CE analysis of nanomolar mixtures of amino acid biosignature molecules has been demonstrated with a fully integrated MOA. The fully automated analysis (Trace iii) separation efficiency ranged from 2.4 $x10^5$ (Arg) to 1.3 $x10^5$ theoretical plates (Gly) and the resolution of Serine – Alanine separation was 1.26. Baseline noise was equivalent of 140 pM Arginine, and the signal-to-noise ratio for single peaks ranged from 141:1 (Arg) to 8:1 (Asp). His and Leu co-migrated, as did Ala and β-Ala in these separation conditions.

The comparison of the manual CE sample loading (Trace i) and the automated pumped CE sample transfer (Trace ii) demonstrated agreement in peak heights to within 8 %, except glutamic acid and aspartic acid, which agreed within 25 %; the reduced agreement for these acidic species was likely due to their lower signal strength and S/N.

The agreement between the bench-labeled sample and the PMA-labeled sample are within 20% for Val, Glu, His/Leu, and Asp. The slightly lower peak height for Ala in the 1-hour automated label reaction is an expected result of its slower labeling kinetics[19]. The increased glycine and serine intensities in the automated label are likely the result of a slightly elevated background of these species during the PMA operation, which was not performed in a HEPA filtered environment.

DISCUSSION

A flight-format Microfluidic Organic Analyzer has been designed, fabricated, and tested, demonstrating successful integrated precise microfluidic sample processing coupled with high resolution CE separation and high sensitivity LIF detection of amino acid biomarkers. While microfluidic CE analysis of organic biomarkers have been performed previously, this is the first demonstration of the functional operation of an integrated system and instrument designed specifically for space flight. MOA automatically measured 20 nM amino acids, equivalent to 0.5 picomole in the analyzed diluted sample. Limits of detection were 0.1 to 5 nM (0.01 to 0.5 ppb), equivalent to 3 to 125 femtomoles for each amino acid in the CE analysis, limited by labeling reaction kinetics.[19] MOA performance therefore exceeded the ~1 picomole sensitivity limit of the SAM GC-MS analyzer on Mars Curiosity rover. Successful functional performance was verified after vibration testing was completed on the manifold with the PMA-CE wafer stack and solenoids integrated, and on the LIF detection system (6.8 g_{rms} Minimum Workmanship, General Environmental Verification Standard[42]). Furthermore, the assembled system was recently tested and successfully operated in zero and high gravity parabolic flight, demonstrating that microfluidics are insensitivity to gravitational variation.[43] While more environmental testing remains to be done, these results demonstrate the advanced Technology Readiness Level or TRL of the MOA system.

The microfluidic PMA processor allows processing and analysis of low-volume samples for many types of chemical species. The central microvalve array is capable of pumping a volume of 850 nanoliters per cycle with minimal dead volume, allowing it to transfer from one analytical function to the next while providing unique programmable flexibility in fluid manipulations.

Importantly, because the PMA-μCE is not limited to a single-function microfluidic device design, it is capable of performing a vast range of both existing and new chemical sample analyses by simply changing the reagents and operational protocol. Electrokinetic injection provides extremely small (picoliter) injection plugs, resulting in very high separation efficiency while requiring just a small fraction of the prepared sample. Therefore, repeat injections are possible, easily achieving confirmatory analyses in minutes. Furthermore, the dynamic range can be adapted to cover unexpectedly high concentrations by dilution on the PMA and by reducing PMT gain factors. Alternatively, the sensitivity can be increased by factors of 10-100 by performing stacking injections at the expense of reduced resolution.[25]

Our results confirm the successful performance of several critical steps for remote autonomous operation in novel extraterrestrial environments. Importantly, fluid transport and mixing ratios are reliably implemented by executing an appropriate number of pump cycles, which is foundational for autonomous operation. Second, aliquots of dry PBSE were successfully stored and rehydrated for each experiment. The labeling efficiency of automated microfluidic mixing with this labeling reagent storage format was essentially unchanged compared with standard bench preparation. Labeled peak intensities are directly related to analyte abundance but the labeling kinetics and efficiency depend on the species being labeled. For instance, labeling efficiencies of arginine, serine, valine and glycine quickly plateau with increased time and labeling reagent, whereas the slower alanine reaction is more sensitive to labeling time and temperature. To address this, we have recently completed a detailed analysis of the interaction of time, temperature, pH and labeling reagent concentration on labeling rate and labeling efficiency for PBSE, resulting in a theory and method for determining the labeling efficiency for any species.[19] This, together with traditional spiking with known analytes, is a powerful approach for

determining the absolute concentrations of both expected and unexpected biomarkers using the Microfluidic Organic Analyzer.

The full analytical capabilities of MOA encompasses functional group-specific fluorescence detection of species separated by their molecular size and charge as demonstrated here, and measurement of enantiomeric excess for chiral biosignatures such as amino acids. We previously developed and field-tested the performance of chiral separations of amino acids by Micellar ElectroKinetic Chromatography (MEKC) using a prototype of the MOA instrument.[18] Using an updated MEKC sample preparation protocol, we recently demonstrated chiral separation of 2 nM D,L-serine and D,L-alanine on the current MOA μCE chip.[44] The updated protocol enables automated MEKC chiral separations to be performed on the same labeled sample analyzed by CE, using an MEKC run buffer. The second dilution step reported in the MOA automated amino acid test demonstrated the process in which an aliquot of labeled sample may be diluted into appropriate run buffer for either CE or MEKC. Thus, automated chiral analyses are easily performed with the same MOA hardware by executing different microfluidic PMA processing sequences.

CONCLUSION

The search for direct chemical evidence of extraterrestrial life in our solar system is perhaps the most profound remaining human question. Interestingly, this quest has been prominent for over 50 years although only the two Viking landers in 1975-76 had a specific objective to search for extraterrestrial life! We now know much more about how life, albeit very dilute, can extend into extreme environments and our analytical detection techniques have been extended to the ultimate limits of molecular detection. The Microfluidic Organic Analyzer presented here

exploits current advancements in technology and understanding to provide a proven a high TRL flight-design instrument that can address this search for life to the meaningful limits currently recognized in the most extreme environments on earth.

REFERENCES

1. Neveu, M.; Hays, L.E.; Voytek, M.A.; New, M.H.; Schulte, M.D. The Ladder of Life Detection. *Astrobiology*. **2018**, *18*, 1375-1402. DOI:10.1089/ast.2017.1773.

2. Biemann, K.; Oro, J.; Iii, P.T.; Orgel, L.E.; Nier, A.O. Search for Organic and Volatile Inorganic Compounds in Two Surface Samples from the Chryse Planitia Region of Mars. *Science*. **1976**, DOI: 10.1126/science.194.4260.

3. Biemann, K.; Oro, J.; Toulmin, P.; Orgel, L.E.; Nier, A.O.; Anderson, D.M. *et al.* The Search for Organic Substances and Inorganic Volatile Compounds in the Surface of Mars. *J Geophys Res*. **1977**, *82*, 4641-4658. DOI:10.1029/js082i028p04641.

4. Squyres, S. *Roving Mars: Spirit, Opportunity, and the Exploration of the Red Planet*. Hachette Books, **2005**. ISBN: 9781401381912

5. Mahaffy, P.R.; Webster, C.R.; Cabane, M.; Conrad, P.G.; Coll, P.; Atreya, S.K. *et al.* The Sample Analysis At Mars Investigation and Instrument Suite. *Space Sci. Rev.* **2012**, *170*, 401-478. DOI:10.1007/s11214-012-9879-z.

6. Freissinet, C.; Glavin, D.P.; Mahaffy, P.R.; Miller, K.E.; Eigenbrode, J.L.; Summons, R.E. *et al.* Organic Molecules in the Sheepbed Mudstone, Gale Crater, Mars. *J. Geophys. Res. Planets*. **2015**, *120*, 495-514. DOI:10.1002/2014je004737.

7. Millan, M.; Teinturier, S.; Malespin, C.A.; Bonnet, J.Y. Organic Molecules Revealed in Mars's Bagnold Dunes by Curiosity's Derivatization Experiment. *Nature*. **2022**, *6*, 129-140. DOI:10.1038/s41550-021-01507-9.

8. Bhartia, R.; Beegle, L.W.; Deflores, L.; Abbey, W.; Razzell Hollis, J.; Uckert, K. *et al.* Perseverance's Scanning Habitable Environments with Raman and Luminescence for Organics and Chemicals (SHERLOC) Investigation. *Space Sci. Rev.* **2021**, *217*, 1-115. DOI:10.1007/s11214-021-00812-z.

9. Hendrix, A.R.; Hurford, T.A.; Barge, L.M.; Bland, M.T.; Bowman, J.S.; Brinckerhoff, W. *et al.* The NASA Roadmap to Ocean Worlds. *Astrobiology*. **2019**, *19*, 1-27. DOI:10.1089/ast.2018.1955.

10. Reh, K.; Spilker, L.; Lunine, J.I.; Waite, J.H.; Cable, M.L.; Postberg, F. *et al.* Enceladus Life Finder: The Search for Life in a Habitable Moon. **2016**, *2016 IEEE Aerospace Conference*, 1-8. DOI:10.1109/AERO.2016.7500813.

11. Mathies, R.A.; Razu, M.E.; Kim, J.; Stockton, A.M.; Turin, P.; Butterworth, A.L. Feasibility of Detecting Bioorganic Compounds in Enceladus Plumes wth the Enceladus Organic Analyzer. *Astrobiology*. **2017**, *17*, 902-912. DOI:10.1089/ast.2017.1660.

12. Hand, K.P.; Murray, A.E.; Garvin, J.B.; Brinckerhoff, W.B.; Christner, B.C.; Edgett, K.S. *et al.* Report of the Europa Lander Science Definition Team. *National Aeronautics and Space Administration.* **2017**.

13. Postberg, F.; Khawaja, N.; Abel, B.; Choblet, G.; Glein, C.R.; Gudipati, M.S. *et al.* Macromolecular Organic Compounds from the Depths of Enceladus. *Nature*. **2018**, *558*, 564-568. DOI:10.1038/s41586-018-0246-4.

14. Mathies, R.A.; New, J.S.; Golozar, M.; Butterworth, A.L. On the Feasibility of Informative Biosignature Measurements Using an Enceladus Plume Organic Analyzer. *Planet. Sci. J.* **2021**, *2*, 163. DOI:10.3847/psj/ac0e9b.

15. Cable, M.L.; Porco, C.; Glein, C.R.; German, C.R.; Mackenzie, S.M.; Neveu, M. *et al.* The Science Case for a Return to Enceladus. *Planet. Sci. J.* **2021**, *2*, 132. DOI:10.3847/psj/abfb7a.

16. Mackenzie, S.M.; Neveu, M.; Davila, A.F.; Lunine, J.I.; Cable, M.L.; Phillips-Lander, C.M. *et al.* Science Objectives for Flagship-Class Mission Concepts for the Search for

Evidence of Life at Enceladus. *Astrobiology*. **2022**, *6*, 685-712. DOI:10.1089/ast.2020.2425.

17. Getty, S.A.; Dworkin, J.P.; Glavin, D.P.; Martin, M.; Zheng, Y.; Balvin, M. *et al.* Organics Analyzer for Sampling Icy Surfaces: A Liquid Chromatograph-Mass Spectrometer for Future in Situ Small Body Missions. *2013 IEEE Aerospace Conference*. **2012**, 1-8. DOI:10.1109/aero.2013.6497391.

18. Chiesl, T.N.; Chu, W.K.; Stockton, A.M.; Amashukeli, X.; Grunthaner, F.; Mathies, R.A. Enhanced Amine and Amino Acid Analysis Using Pacific Blue and the Mars Organic Analyzer Microchip Capillary Electrophoresis System. *Anal. Chem.* **2009**, *81*, 2537-2544. DOI:10.1021/ac8023334.

19. Casto-Boggess, L.D.; Golozar, M.; Butterworth, A.L.; Mathies, R.A. Optimization of Fluorescence Labeling of Trace Analytes: Application to Amino Acid Biosignature Detection wth Pacific Blue. *Anal. Chem.* **2022**, *94*, 1240-1247. DOI:10.1021/acs.analchem.1c04465.

20. New, J.S.; Kazemi, B.; Spathis, V.; Price, M.C.; Mathies, R.A.; Butterworth, A.L. Quantitative Evaluation of the Feasibility of Sampling the Ice Plumes at Enceladus for Biomarkers of Extraterrestrial Life. *Proc. Natl. Acad. Sci. USA*. **2021**, *118*, e2106197118. DOI:10.1073/pnas.2106197118.

21. Convery, N.; Gadegaard, N. 30 Years of Microfluidics. *Micro and Nano Engineering*. **2019**, *2*, 76-91. DOI:10.1016/j.mne.2019.01.003.

22. Manz, A.; Neuzil, P.; O'connor, J.S.; Simone, G. *Microfluidics and Lab-on-a-chip*. Royal Society of Chemistry, **2020**. ISBN: 9781782628330

23. Cheng, Y.-F.; Dovichi, N.J. Subattomole Amino Acid Analysis By Capillary Zone Electrophoresis and Laser-Induced Fluorescence. *Science*. **1988**, *242*, 562-564. DOI:10.1126/science.3140381.

24. Amankwa, L.N.; Albin, M.; Kuhr, W.G. Fluorescence Detection in Capillary Electrophoresis. *TrAC Trends in Analytical Chemistry*. **1992**, *11*, 114-120. DOI:10.1016/0165-9936(92)85009-t.

25. Skelley, A.M.; Scherer, J.R.; Aubrey, A.D.; Grover, W.H.; Ivester, R.H.C.; Ehrenfreund, P. *et al.* Development and Evaluation of a Microdevice for Amino Acid Biomarker Detection and Analysis on Mars. *Proc. Natl. Acad. Sci.* **2005**, *102*, 1041-1046. DOI:10.1073/pnas.0406798102.

26. Hutt, L.D.; Glavin, D.P.; Bada, J.L.; Mathies, R.A. Microfabricated Capillary Electrophoresis Amino Acid Chirality Analyzer for Extraterrestrial Exploration. *Anal. Chem.* **1999**, *71*, 4000-4006. DOI:10.1021/ac9903959.

27. Skelley, A.M.; Cleaves, H.J.; Jayarajah, C.N.; Bada, J.L.; Mathies, R.A. Application of the Mars Organic Analyzer to Nucleobase and Amine Biomarker Detection. *Astrobiology*. **2006**, *6*, 824-837. DOI:10.1089/ast.2006.6.824.

28. Stockton, A.M.; Tjin, C.C.; Huang, G.L.; Benhabib, M.; Chiesl, T.N.; Mathies, R.A. Analysis of Carbonaceous Biomarkers wth the Mars Organic Analyzer Microchip Capillary Electrophoresis System: Aldehydes and Ketones. *Electrophoresis*. **2010**, *31*, 3642-3649. DOI:10.1002/elps.201000424.

29. Stockton, A.M.; Tjin, C.C.; Chiesl, T.N.; Mathies, R.A. Analysis of Carbonaceous Biomarkers wth the Mars Organic Analyzer Microchip Capillary Electrophoresis System: Carboxylic Acids. *Astrobiology*. **2011**, *11*, 519-528. DOI:10.1089/ast.2011.0634.

30. Mora, M.F.; Stockton, A.M.; Willis, P.A. Analysis of Thiols By Microchip Capillary Electrophoresis for in Situ Planetary Investigations. *Electrophoresis*. **2013**, *34*, 309-316. DOI:10.1002/elps.201200379.

31. Willis, P.A.; Creamer, J.S.; Mora, M.F. Implementation of Microchip Electrophoresis Instrumentation for Future Spaceflight Missions. *Anal. Bioanal. Chem.* **2015**, *407*, 6939-6963. DOI:10.1007/s00216-015-8903-z.

32. Skelley, A.M.; Aubrey, A.D.; Willis, P.A.; Amashukeli, X.; Ehrenfreund, P.; Bada, J.L. *et al.* Organic Amine Biomarker Detection in the Yungay Region of the Atacama Desert

with the Urey Instrument. *J Geophys Res Biogeosci*. **2007**, *112*, G04S11. DOI:10.1029/2006jg000329.

33. Mora, M.F.; Kehl, F.; Costa, E.T.D.; Bramall, N.; Willis, P.A. Fully Automated Microchip Electrophoresis Analyzer for Potential Life Detection Missions. *Anal. Chem.* **2020**, *92*, 12959-12966. DOI:10.1021/acs.analchem.0c01628.

34. Stockton, A.M.; Chiesl, T.N.; Lowenstein, T.K.; Amashukeli, X.; Grunthaner, F.; Mathies, R.A. Capillary Electrophoresis Analysis of Organic Amines and Amino Acids in Saline and Acidic Samples Using the Mars Organic Analyzer. *Astrobiology*. **2009**, *9*, 823-831. DOI:10.1089/ast.2009.0357.

35. Skelley, A.M.; Grunthaner, F.J.; Bada, J.L.; Mathies, R.A. Mars Organic Detector III: A Versatile Instrument for Detection of Bio-Organic Signatures on Mars. *First Jet Propulsion Laboratory In Situ Instruments Workshop*. **2003**, *4878*, 59-67. DOI:doi.org/10.1117/12.520580.

36. Kim, J.; Jensen, E.C.; Stockton, A.M.; Mathies, R.A. Universal Microfluidic Automaton for Autonomous Sample Processing: Application to the Mars Organic Analyzer. *Anal. Chem.* **2013**, *85*, 7682-7688. DOI:10.1021/ac303767m.

37. Golozar, M.; Chu, W.K.; Casto, L.D.; Mccauley, J.; Butterworth, A.L.; Mathies, R.A. Fabrication of High-Quality Glass Microfluidic Devices for Bioanalytical and Space Flight Applications. *MethodsX*. **2020**, *7*, 101043. DOI:10.1016/j.mex.2020.101043.

38. Chu, W.K., Mathies: Wafers Cleaning and Deposition, *https://openwetware.org/wiki/Mathies:Wafers_Cleaning_and_Deposition*, **2009**.

39. Paegel, B.M.; Hutt, L.D.; Simpson, P.C.; Mathies, R.A. Turn Geometry for Minimizing Band Broadening in Microfabricated Capillary Electrophoresis Channels. *Anal. Chem.* **2000**, *72*, 3030-3037. DOI:10.1021/ac000054r.

40. Estlack, Z.; Compton, B.; Razu, M.E.; Kim, J. A Simple and Reliable Microfabrication Process for a Programmable Microvalve Array. *MethodsX*. **2022**, *9*, 101860. DOI:10.1016/j.mex.2022.101860.

41. Estlack, Z.; Kim, J. Microvalve Array Fabrication Using Selective Pdms (Polydimethylsiloxane) Bonding Through Perfluorooctyl-Trichlorosilane Passivation for Long-Term Space Exploration. *Scientific Reports*. **2022**, *12*, 12398. DOI:10.1038/s41598-022-16574-9.

42. General Environmental Verification Standard (GEVS) for GSFC Flight Programs and Projects. URL: https://standards.nasa.gov/standard/gsfc/gsfc-std-7000. **2021**.

43. Estlack, Z.; Golozar, M.; Butterworth, A.L.; Mathies, R.A.; Kim, J., *npj Microgravity* (2023), in press.

44. Butterworth, Anna L.; Golozar, M.; Spathis, V.; Casto-Boggess, L.; Mathies, R.A. Survival of Chiral Amino Acids Captured in High Velocity Enceladus Ice Plume Analog Impact Experiments. *Fall Meeting 2022. AGU*. **2022**.

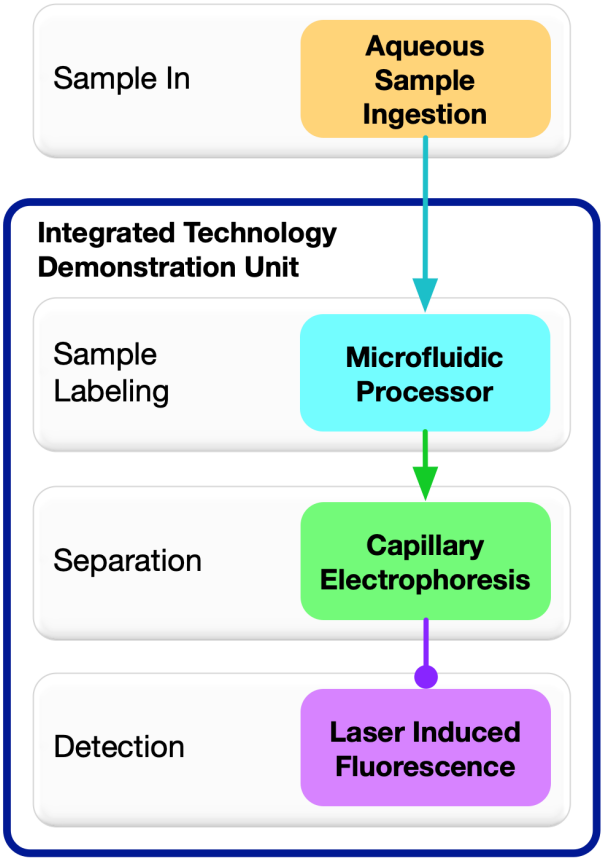

Figure 1: Schematic overview of the Microfluidic Organic Analyzer instrument and analysis process. Microliter-aqueous sample from a sample handling system is pumped into the microfluidic processor and mixed with reagents so that analytes are selectively fluorescently labeled. After incubation, the labeled sample is transferred to the CE sample well for electrokinetic injection, separation and confocal LIF detection to reveal molecular identity and concentration.

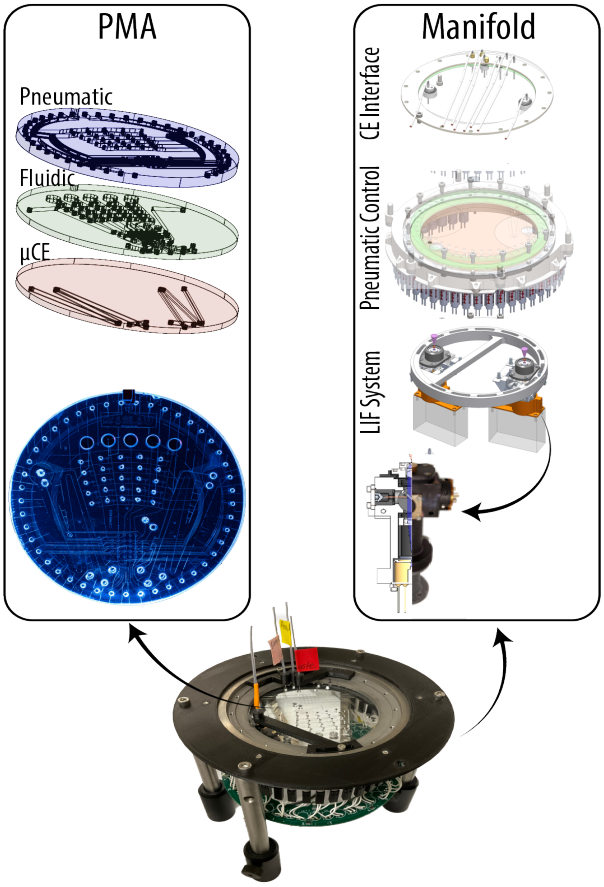

Figure 2*:* Flight format PMA-CE-LIF instrument design and hardware. Left: Programmable Microfluidic Analyzer (PMA), with expanded view (from top) showing the pneumatic and fluidic PDMS layers and the glass µCE channels, and plan view of the bonded 10-cm diameter microfabricated device. Right: expanded manifold components, including (from top) CE interface and pressure chamber lid, pneumatic manifold with latching solenoids, dual CE-LIF detection system and LIF detector split view showing confocal optical design and fabricated hardware. Center: Photograph of the fabricated PMA-CE-LIF instrument, shown functioning without pressure lid installed.

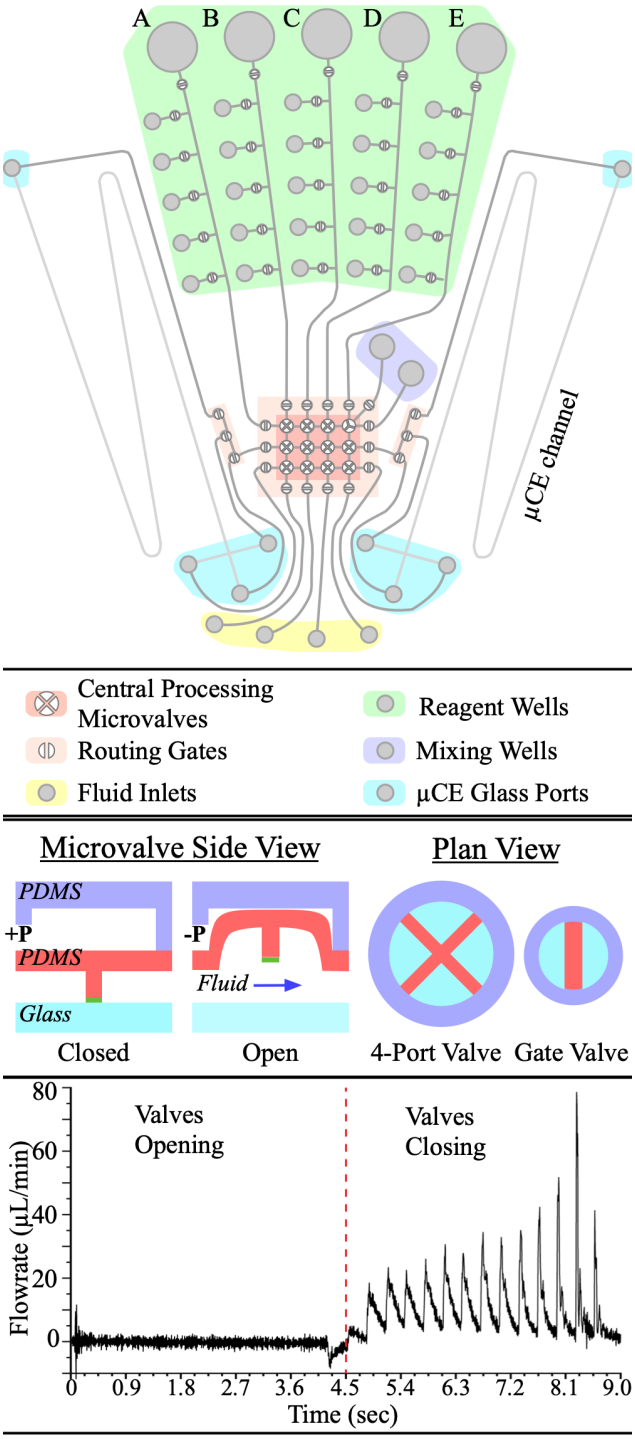

Figure 3. Schematic of the integrated Programmable Microfluidic Analyzer – microfabricated Capillary Electrophoresis (PMA-µCE) device. Top: PMA placement of microvalves, channels and fluid reservoirs connected to two glass µCE channels. Shaded areas denote the fluid wells.

Middle: Pneumatic microvalve structure with side views showing closed and open states and plan views showing the 4-way Central Processing Microvalves (CPM) valves and 2-way routing gates. Bottom: Measured flowrate during one metered pumping cycle showing sequential opening to fill 12 CPM valves followed by closing to empty the CPM.

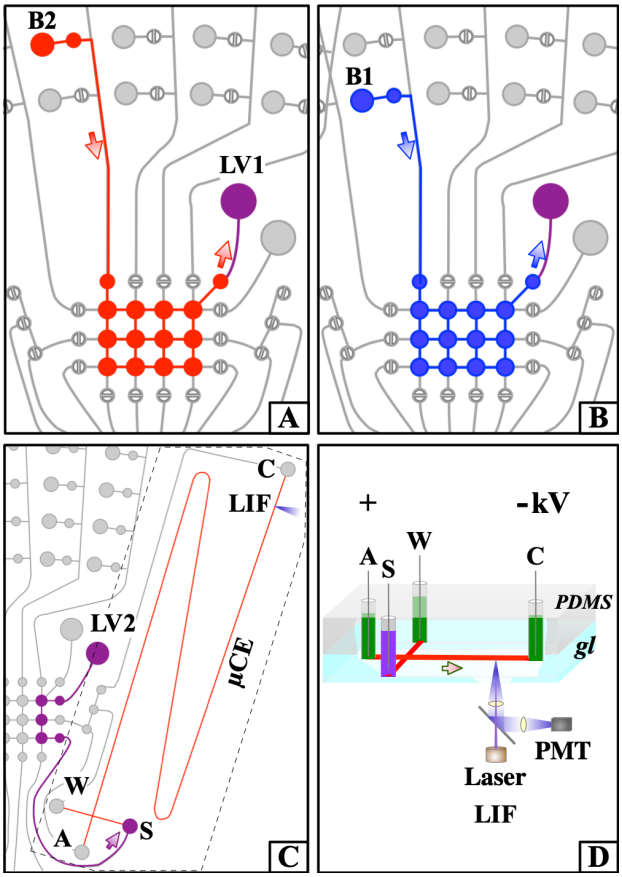

Figure 4. Illustration of the **PMA** fluidic routing used in the process of performing an amino acid (AA) analysis. Panels A and B: Efficient mixing by alternating the amino acid solution (*B2,* red) with Pacific Blue (PB) in 2X buffer (*B1,* blue) for labeling in an incubation well (*LV1).* The process is repeated 10 times to create a 1:1 mixture, total volume 13 µL. Panel C: The labeled sample in *LV1* has been diluted with CE buffer in a similar manner into *LV2.* The diluted sample (purple) is transferred from *LV2* to the CE Sample well, *CS2* for CE-LIF analysis in the folded 15 cm µCE channel (red). Panel D: cut-away view of µCE-LIF (glass and PDMS fluid layer not to scale), with **S**ample (purple fluid), **A**node, **W**aste and **C**athode (green fluid) ports connected to

the μCE cross channel (red), Pt electrodes inserted to each fluid well, and the LIF mounted beneath.

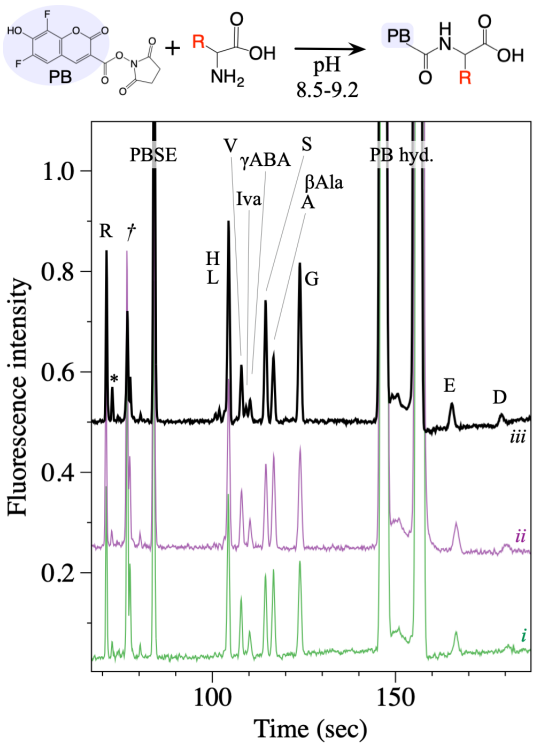

Figure 5. Electropherograms demonstrating automated labeling, loading and integrated CE-LIF analysis of an amino acid mixture using the flight format PMA-CE organic analyzer. The PB labeling reaction scheme is shown at top. The amino acid concentrations were 50 nM Arg, His, Leu, Val, γABA, S, βAla, Ala, Gly, and 100 nM Iva, Glu, and Asp with 50 µM Pacific Blue PBSE at 25° C. The traces are normalized to 20 nM Arg injected concentration. Trace i was bench prepared and analyzed by manual filling of the CE sample reservoir. Trace ii was obtained by filling *LV2* with the bench-prepared sample and pumping the sample to the CE for analysis. The fully automated labeling and integrated analysis is shown in Trace *iii*. Amino acid peak assignments using standard one-letter codes are shown plus *PBSE* unreacted dye, *PB hyd* hydrolyzed dye; CE conditions were 60 second pre-clean (-1000 V at Sample and Waste), 40 seconds electrokinetic injection (-1000 V at Waste) and 467 V/cm separation and -640 V back bias at Sample and Waste. *Indicates PBSE reagent contaminants e.g. lysine, †ethanolamine and ethylamine.

ASSOCIATED CONTENT

Supporting Information.

For additional information see http://eoa.ssl.berkeley.edu

Supplemental Tables and Figures

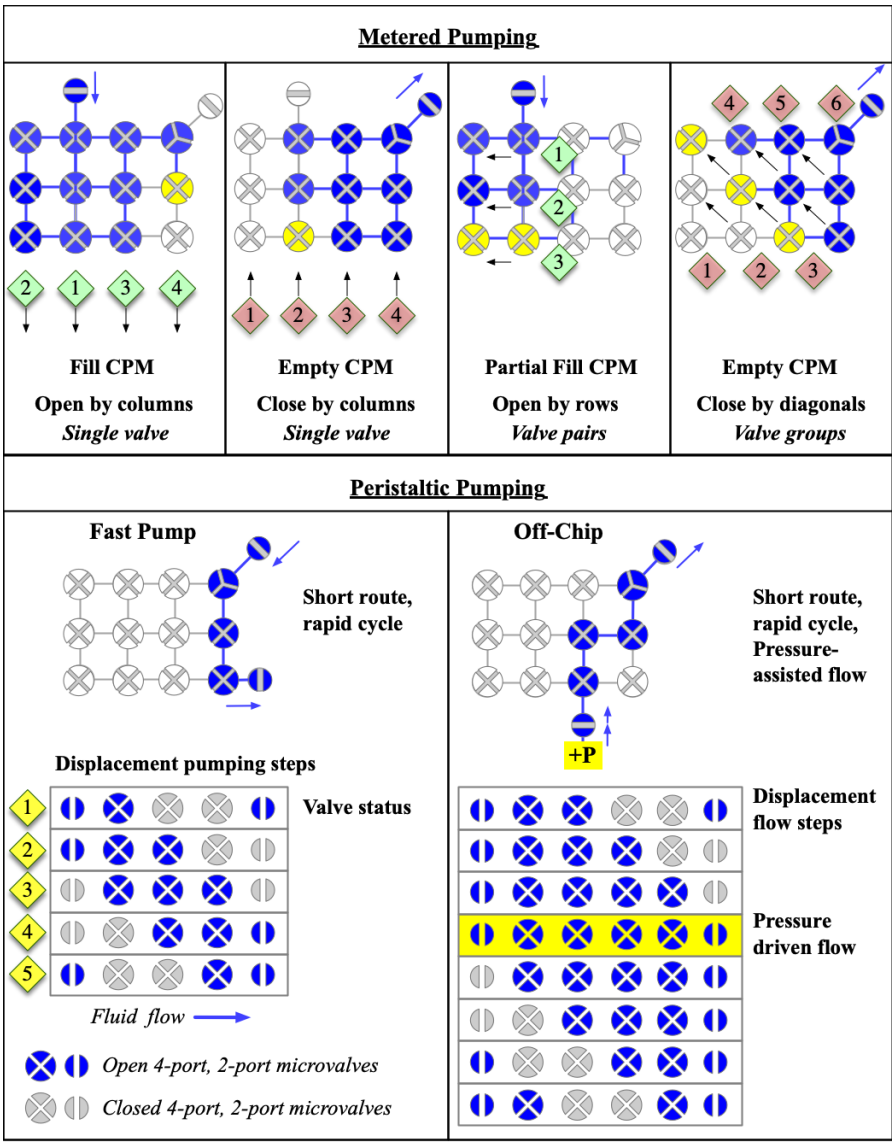

Figure S1. Sequential actuations of the central processor microvalves (CPM) enable a wide variety of precise user-defined protocols on the same hardware device. Black arrows denote the order of microvalve actuation during each fluidic step; green diamonds show the order of opening a group of valves (by column, row or diagonal); red diamonds show the order of closing by group; yellow-shaded valves indicate the next actuations in the sequence. The blue arrows show the direction of fluid flow (in or out the CPM array).

Slower filling and emptying of the CPM is used for **metered pumping** for precise volume displacement. A user defined fraction of the CPM valves can be employed to define the fluid volume to be displaced and one-by-one valve actuations provide reliable mixing ratios. Single source processing can employ actuation of 2 or 3 valves switched rapidly as a group to speed up rinsing or priming processes; actuations separated by the 30 ms solenoid switching time are treated as simultaneous with respect to fluid flow control. Times delays between single or group valve actuations are typically 100 to 600 ms.

Lower panel: A fluid bolus is pumped as a wave through a short path in the CPM in **peristaltic pumping**, by switching valve status for each step shown in the table to complete one cycle. Two options are shown for fast on-chip transfer and for ingesting fluid from off-chip using pressure-assisted displacement pumping. In the off-chip example, a "leak" step is inserted (highlighted in yellow), during which all four CPM valves and the two routing gate valves open a path directly to the destination allowing pressure driven flow but for less than 1 second per cycle. Adding a small head pressure to the off-chip fluid supply (10 kPa above ambient, well below the breakthrough pressure for the PDMS microvalve structures) overcomes fluid resistance and significantly speeds up the flow, while the displacement pumping provides precision and safety.

In this way, off-chip volume and delivery rates are user-defined, without risk of overfilling chip reservoirs.

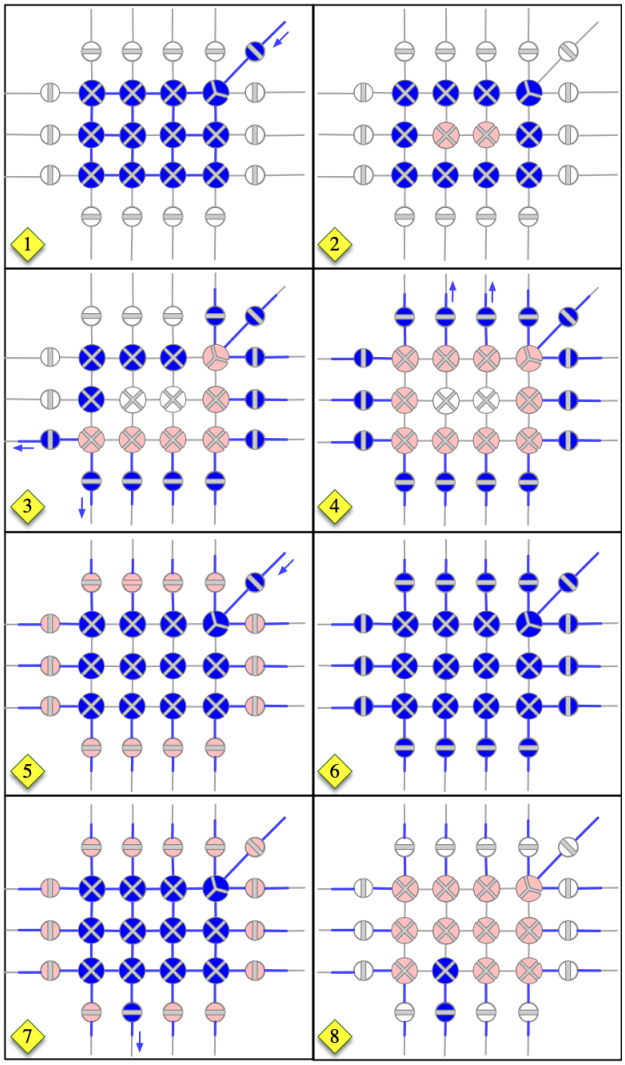

Figure S2. Steps for priming the CPM by pumping in water from *LV1* emptying each time to *Waste* (off-chip). Panel 1: the CPM valves are filled from LV1. Panel 2: preparing to prime the peripheral gate valves, the two central CPM valves are closed. Panels 3 and 4 take 1 second to complete, wherein each remaining CPM valve expels through the attached gate(s). In Panel 5, the gate valves are all closed so that the CPM can be refilled. Panels 2 to 4 are typically repeated 3 times, taking ~30 seconds after which ~200 nL fluid has been pumped to fill each gate valve

plus a small length of channel behind each one (preventing air being sucked back to the CPM). In Panel 6, the CPM is held open for 2 minutes to allow the fluid to degas through the PDMS membrane into the vacuum above each valve in the pneumatic layer, taking about 4 minutes total to complete prime the chip from dry until ready for use. Panel 7: It takes 2 seconds to close the gate valves and empty the CPM to Waste, ending with the last valve to close shown in Panel 8, and the chip is ready for immediate use.

Table S1 Automated Sample Preparation and Analysis Steps

Microfluidic Step	Pump Cycle	Repeat	Source	#	Destination	Fill time	Empty time
Priming route with buffer							
Prime Well B1	B6 to B1	1	B6	6	B1	800	400
Prime Well B2	R6B to R2B	1	B6	6	B2	800	400
Prime Well LV1	R6B to LV1	1	B6	12	LV1	800	400
Mix Sample and Dye to label (1:1)							
Mix Sample	B2 to LV1	10	B2	12	LV1	800	400
Mix Dye/Buffer	B1 to LV1		B1	12	LV1	800	400
Dilute labeled sample with CE running buffer (2:3)							
Add Buffer	B6 to LV2	5	B6	12	LV2	800	400
Mix Sample	LV1 to LV2	10	LV1	12	LV2	800	400
Mix Buffer	B6 to LV2		B6	12	LV2	800	400
Transfer labeled sample to CE Sample well							
Transfer to CE	LV2 to CS2	15	LV2	12	CS2	600	400

AUTHOR INFORMATION

Corresponding Author

* Address correspondence to Dr. Anna Butterworth at the Space Sciences Laboratory, UC Berkeley,

butterworth@berkeley.edu

Author Contributions

The manuscript was prepared through contributions of all authors who have given approval to the final version. R. Mathies and A. Butterworth developed the project ideas and provided oversight on all aspects of instrument fabrication and demonstration. J. McCauley was predominantly responsible for instrument fabrication and assembly. J. Kim and Z. Estlack designed, microfabricated, and validated the PMA and integrated PMA-CE. A. Butterworth developed integrated functional tests and automated analyses. M. Golozar provided expert glass CE wafer fabrication and analysis expertise.

Funding Sources

This research was supported by the National Aeronautics and Space Administration (NASA) under grant No. 80NSSC 17K0600 issued by the SMD/Planetary Science Division through the MatISSE Program and by 80NSSC19K0616 issued by the SMD/Planetary Science Division through the ICEE-2 Program.

Notes

The authors declare that they have no financial interests that might influence the work reported in this paper.

ACKNOWLEDGMENTS

This research was supported by the National Aeronautics and Space Administration (NASA) under grant No. 80NSSC 17K0600 issued by the SMD/Planetary Science Division through the MatISSE Program and by 80NSSC19K0616 issued by the SMD/Planetary Science Division through the ICEE-2 Program. Z. Estlack and J. Kim acknowledge additional financial support from the University of Utah. This research was conducted in part at the Utah Nanofab sponsored by the College of Engineering, office of the Vice President for Research, and the Utah Science Technology and Research (USTAR) initiative of the State of Utah.

ABBREVIATIONS

PMA, programmable microfluidic analyzer; CE, capillary electrophoresis; AA, amino acid; PB, Pacific Blue; MOA, microfluidic organic analyzer; PDMS, poly dimethyl silane; CE capillary electrophoresis; LIF laser induced fluorescence